ACS Chemical Neuroscience

LETTER

pubs.acs.org/acschemicalneuroscience

Molecular Engineering of a Secreted, Highly Homogeneous, and Neurotoxic Aβ Dimer

Andreas Müller-Schiffmann,[†] Aksana Andreyeva,[‡] Anselm H. C. Horn,[§] Kurt Gottmann,[‡] Carsten Korth,[*,†] and Heinrich Sticht[*,§]

[†]Department Neuropathology and [‡]Department Neurophysiology, Heinrich Heine University, Düsseldorf, Germany

[§]Institute of Biochemistry, University of Erlangen-Nürnberg, 91054 Erlangen, Germany

Supporting Information

ABSTRACT: Aβ oligomers play a key role in the pathophysiology of Alzheimer's disease. Research into structure−function relationships of Aβ oligomers has been hampered by the lack of large amounts of homogeneous and stable material. Using computational chemistry, we designed conservative cysteine substitutions in Aβ aiming at accelerating and stabilizing assembly of Aβ dimers by an intermolecular disulfide bond without changing its folding. Molecular dynamics simulations suggested that mutants AβS8C and AβM35C exhibited structural properties similar to those of Aβ wildtype dimers. Full length, mutant APP was stably expressed in transfected cell lines to study assembly of Aβ oligomers in the physiological, secretory pathway and to avoid artifacts resulting from simultaneous in vitro oxidation and aggregation. Biochemical and neurophysiological analysis of supernatants indicated that AβS8C generated an exclusive, homogeneous, and neurotoxic dimer, whereas AβM35C assembled into dimers, tetramers, and higher oligomers. Thus, molecular engineering enabled generation of bioactive, homogeneous, and correctly processed Aβ dimers in vivo.

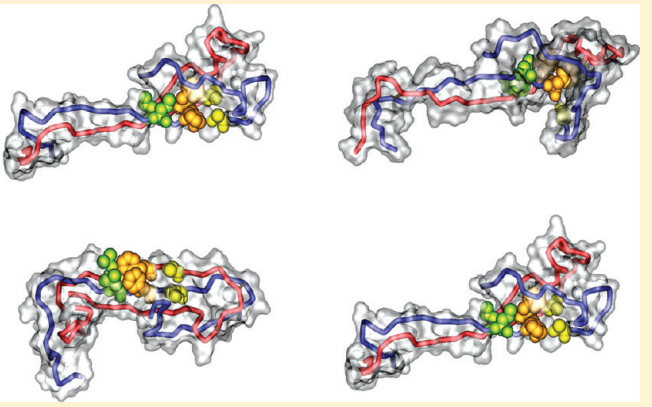

KEYWORDS: Alzheimer's disease, computational chemistry, Aβ oligomers, dimers, molecular engineering, neurotoxicity

Alzheimer's disease (AD) is the most prevalent neurodegenerative disorder with the amyloid-β-peptide (Aβ) playing a central role in its pathogenesis.[1] Aβ is generated as a 38−43 residue peptide from the amyloid precursor protein (APP) by the proteolytic activity of β- and γ-secretases.[2,3] Aβ assembles into oligomers of various sizes and Aβ plaques, a neuropathological hallmark of AD.[1] Unlike Aβ fibrils or plaques, only the presence of Aβ oligomers correlates with the cognitive status of AD.[4,5] Aβ oligomers cause synaptic pathology[1,6] in line with findings that loss of dendritic spines correlates to early morphological changes in AD patients.[7]

Many different oligomeric Aβ species have been identified,[8−10] and neurotoxicity has been attributed to Aβ dimers,[6] Aβ dodecamers,[10,11] or others. A recent study from Shankar et al.[6] has provided solid evidence that natively secreted Aβ dimers purified from post-mortem brains of patients with clinical AD are the predominant species sufficient to cause synaptic pathology. To gain insight into structure−function relationships of Aβ dimers, it is of paramount importance to generate or purify highly homogeneous, distinct species of Aβ oligomers. So far, detailed structural investigations of native Aβ oligomers have been hampered by their low abundance in available transgenic mouse models of AD or AD patient brains, and laborious purification procedures.

Synthetic Aβ has been a convenient tool for studying Aβ protein biochemistry, since it can be generated to relatively high purity in large amounts and is therefore readily available for biophysical and structural studies of some aspects of Aβ. However, evidence has accumulated suggesting that synthetic Aβ oligomers are only insufficiently modeling naturally secreted Aβ oligomer functions, even if refolded and purified by laborious procedures. Several studies clearly indicate that the bioactivity of naturally secreted Aβ oligomers from transfected cells is similar to that of AD brain-derived Aβ oligomers, but more than hundred times stronger than that of synthetic Aβ oligomers, when long-term potentiation (LTP) effects are taken as readout.[12] The major difference between natively secreted and synthetic Aβ is that natively secreted Aβ is the result of a highly controlled and quality-checked, cofactor-assisted proteolytic process at low local concentrations, while bulk refolding of synthetic Aβ occurs without regulating cofactors at high local concentrations. Bulk refolding leads to conformational heterogenetiy of refolded Aβ oligomers correlating with different neurotoxicities.[13]

Received: February 20, 2011
Accepted: March 11, 2011
Published: March 11, 2011

A function of natively secreted Aβ oligomers is not established. Their specific effects on AMPA-receptor-related neurotransmission argue in favor of a role in glutamate-related synaptic functions. In bioassays, measuring the effect of AMPA-receptor related neurotransmission such as LTP, synthetic Aβ of same concentrations as natively secreted Aβ consistently is less active.[12] This could indicate that natively secreted and synthetic Aβ oligomers are not exactly in the same conformations and that yet undetermined factors assist in Aβ oligomer assembly during cellular processing.

Structure−function studies of natively secreted Aβ oligomers are difficult owing to their relatively low population on the Aβ aggregation pathway and their heterogeneity with respect to the oligomerization state. Therefore, engineered disulfide-bonds have been introduced into synthetic Aβ to study Aβ toxicity and oligomerization properties.[14,15] In these studies, one or two cysteines were introduced into the Aβ polypeptide chain, leading to either inter- or intramolecular disulfide bonds after oxidation.[14,15] However, when introducing intermolecular disulfide bonds in cell-free synthetic Aβ, the oxidative bond formation and Aβ-aggregation are competing processes, and the fast development of fibrils or insoluble aggregation no longer allows disulfide-bond formation to stabilize soluble oligomers. The conditions for oxidation of synthetic peptides need to be critically controlled, and the resulting disulfide-linked oligomers need to be separated from the remaining aggregates.

RESULTS AND DISCUSSION

Although previous approaches allowed the production of stabilized oligomers for in vitro experiments, they are not suitable to predict or study the effects of enhanced native Aβ oligomer production in cell culture or in an animal model. Therefore, alternative avenues to generate stabilized Aβ oligomers are highly desirable. Using computational chemistry, we have rationally designed three cysteine mutants (S8C, S26C, and M35C) to stabilize Aβ oligomers by intermolecular disulfide bonds. The precise sites of the mutations were designed to allow dimer formation already in early stages of the Aβ-processing pathway, and molecular dynamics simulations indicated that the mutations S8C and M35C exhibited structural properties similar to Aβ wildtype dimers. For studying the ordered genesis of Aβ oligomers under cell physiological conditions in the secretory pathway, and to avoid any artifacts resulting from simultaneous in vitro oxidation and aggregation, these mutations were cloned into full length APP and stably expressed in CHO cells by a retroviral inducible system.

At outlined above, the aim of the computational chemistry work was to identify positions in the Aβ sequence which allow the mutation to cysteine without disrupting the Aβ fold. Therefore, we exclusively considered conservative types of side chain replacements (Ser → Cys, Met → Cys). Based on this criterion, three different mutations (S8C, S26C, and M35C) were selected and further analyzed as described in detail below:

(I) Since the Aβ peptide emerges from processing of amyloid precursor protein (APP), compatibility of mutations with the APP secretory pathway was tested. Mutations S26C and M35C are located adjacent to the main APP-dimerization motif spanning G29−G33 of Aβ[16] (Figure 1a). Therefore, Cys-mediated dimerization at position 26 or 35 was expected to be favored in APP itself due to the spatial proximity of these residues in the APP dimer and due to the conservative type of amino acid replacement. Residue 8 of Aβ is located in the extracellular region of APP. Here, the oxidative conditions of the extracellular environment should favor dimerization at this sequence position.

(II) After cleavage of APP, the Aβ peptide undergoes an α-helix to β-sheet conversion (Figure 1b), resulting in dimeric Aβ species, which are characterized by a high amount of parallel β-sheets. Therefore, for all designed disulfide bonds, molecular modeling was used to confirm their consistency with parallel in-register β-sheet formation.

(III) Aβ dimers are generally conformationally heterogeneous, and the elongation-competent U-shaped topology, which is also found in the fibril, is in conformational equilibrium with other elongation incompetent conformations (Figure 1c). The disulfide bond should not favor fibrillation at the expense of the formation of stable dimers. This aspect was addressed by molecular dynamics (MD) simulations. These simulations revealed that the elongation-competent U-shaped topology was

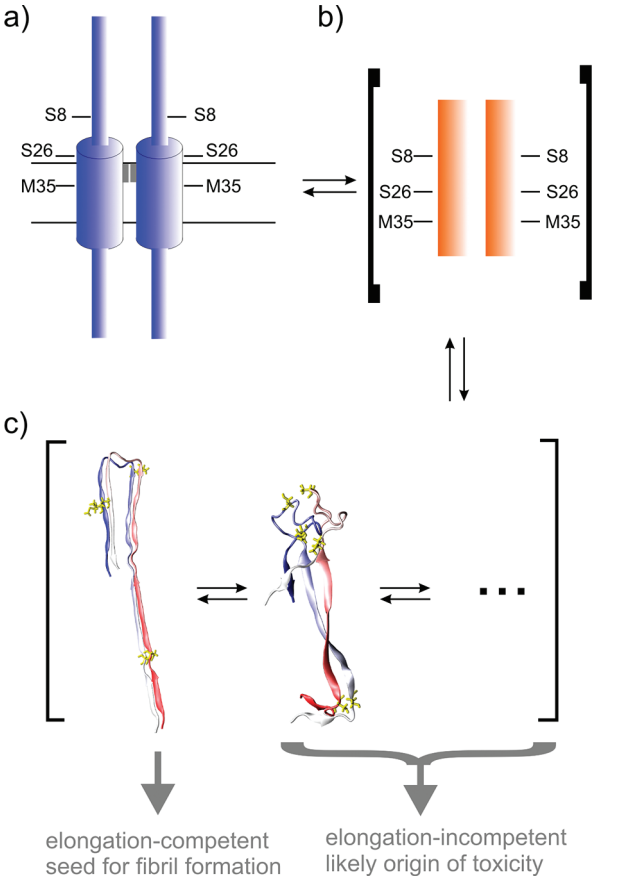

Figure 1. Schematic presentation of the Aβ processing and aggregation pathway depicting the sites of Aβ mutations investigated. (a) APP dimer showing that S26 and M35 are located in the transmembrane helix close to the G29−G33 dimerization motif (shown as gray rectangle). S8 is located in the extracellular part of APP. (b) After processing of APP, Aβ undergoes an α-helix to β-sheet conversion and predominantly associates via parallel β-sheets (schematically shown as orange bars). The dimers are generally conformational heterogeneous (c), and the elongation competent U-shaped conformation (left) is in equilibrium with alternative folds (middle, right), which are rather elongation-incompetent and are the most likely candidates for toxic Aβ dimers.

dx.doi.org/10.1021/cn200011h |ACS Chem. Neurosci. 2011, 2, 242–248

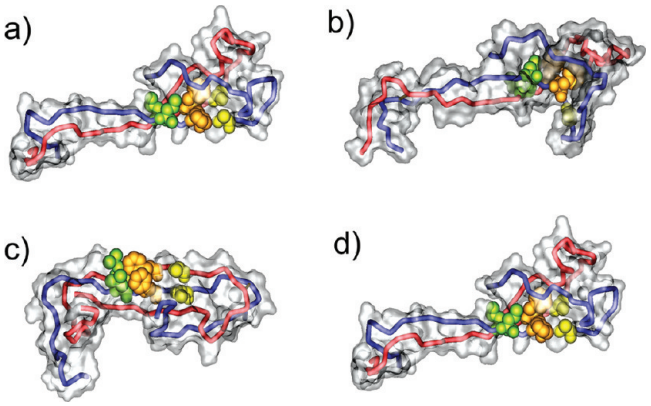

Figure 2. Molecular structure of the most populated Aβ conformation for wildtype (a), S8C (b), S26C (c), and M35C (d) that was present in the respective molecular dynamics simulations. The two chains of the Aβ dimer are shown as red and blue tubes. Residues L17 (green), F19 (orange), and A21 (yellow) of the central hydrophobic core are shown as a space-filled presentation. To emphasize the different degree of solvent accessibility of these core residues, the molecular surface of all remaining residues is shown as a translucent surface. See Supporting Information Table 1 for a detailed analysis of the solvent accessibility.

stable neither in the wildtype nor in the disulfide-bonded mutants investigated (see Supporting Information information for details). Wildtype Aβ and two of the mutants (Aβ S8C, M35C) underwent major changes in their C-terminus and preferentially adopted a conformation exhibiting an additional antiparallel β-sheet in one of the subunits (Figure 2, Supporting Information Figure S2). This conformational rearrangement, which allows efficient shielding of hydrophobic residues from the solvent, had already been detected in previous theoretical studies of wildtype Aβ(9−42).[17,18] Interestingly, the C26 disulfide bond appeared incompatible with the formation of a hydrophobic core formed in the wildtype and S8C/M35C mutants. For the S26C mutant, a planar arrangement was formed that is stabilized by a novel interchain antiparallel β-sheet (Figure 2c).

In summary, we conclude from these simulations that none of the mutants should enhance fibril formation and that the S8C- and M35C-dimers should exhibit structural properties similar to wildtype.

When expressed in CHO cells, the APP(AβS8C) mutant produced exclusively dimeric Aβ but no SDS-resistant oligomers of higher order (Figure 3a, c); the concentration of Aβ dimers was determined by ELISA to be around 2 ng/mL cell culture. No oligomeric Aβ was detected using the APP(AβS26C) cell line, whereas the APP(AβM35C) mutant assembled into dimers, SDS-resistant tetramers, and higher order oligomers (Figure 3a−c). Aβ was absent in the mock control, and only monomeric Aβ was immunoprecipitated from supernatants (SNs) of APP-wt expressing cells. Remarkably, part of the Aβ oligomers and tetramers were reductant-insensitive (Figure 3b); this property was also observed for wildtype Aβ oligomers and is considered a hallmark of neurotoxicity.[9,10] These results suggested that key structural features of wildtype Aβ oligomers were preserved in the presence of the disulfide bond.

Immunoprecipitates of APP(AβM35C) SNs yielded signals in the range of dimers, tetramers, and higher order oligomers at about 60 kDa (∼14-mers; Figure 3a and b). This particular type of association might be favored for M35C because this mutation stabilizes the C-terminal parallel β-sheet characteristic for Aβ-globulomers corresponding to 12−16 peptides/soluble aggregate.[19]

To investigate the homogeneity of the Aβ oligomers under native conditions, we purified the secreted Aβ oligomers by size exclusion chromatography (SEC) and Western blotted the fractions. By performing this analysis, we demonstrated that APP(AβS8C) was processed to yield exclusively dimeric Aβ (Figure 3c), whereas the M35C was assembling to a greater variety of high molecular weight species similar to the results in SDS-PAGE/Western blotting (Figure 3a, c). These findings demonstrated that the exact location of the disulfide bridge had a dramatic effect on the amount and sizes of Aβ oligomers formed.

When we investigated lysates of cells transfected with different APP constructs, it became obvious that dimerization already occurred at the level of APP in the respective Aβ polypeptide region (Figure 4a). These data are consistent with the notion that APP dimerization is critical for correct processing[20,21] and suggest that Aβ processing and Aβ oligomer assembly are more closely linked than previously appreciated. Decreased cell surface staining for APP(AβS26C)-expressing cells with unaffected intracellular staining indicated aberrant proteolytic processing with degradation of APP(AβS26C) before reaching the cell surface (Supporting Information Figure S3). Similar results have been reported for the close-by APP Aβ K28C mutation.[22] In contrast, the presence of APP(AβS8C) and M35C surface staining as well as the binding of Aβ dimers in the SN to mAB IC16 (epitope at residues 2−8 of Aβ; ref 23), reversible by an γ-secretase inhibitor, indicated correct proteolytic processing of APP(AβS8C) and APP(AβM35C).

One of the most sensitive tests for Aβ mediated synaptic pathology is the decrease of AMPA receptor-mediated miniature excitatory postsynaptic currents (mEPSCs) in primary mouse cortical neurons[6,24] that has also been validated for recombinantly expressed and secreted Aβ oligomers from CHO cells.[23] When SNs of mock, human wild type APP, and human APP(AβS8C)-transfected CHO cells were probed on primary mouse neuron mEPSCs, only SN containing AβS8C dimers but not control SN showed a significant decrease in both mEPSC frequency and amplitude (Figure 4b, Supporting Information Figure S4), consistent with the exclusive presence of dimers in the AβS8C species. In another assay testing the biological activity of Aβ oligomers, treatment of NGF-differentiated PC12 cells with Aβ derived from APP(AβS8C) and APP(AβM35C) transfected and induced cell lines but not control SNs resulted in a markedly reduced growth of neurites (Figure 4c).

The enhanced dimer formation and toxicity observed for AβM35C shows that introduction of a disulfide bond confers strikingly different molecular properties compared to M35 oxidation. Oxidation of M35 significantly changes the polarity and spatial requirement of the methionine residue, thereby lowering the assembly kinetics and toxicity of Aβ.[25,26] However, our in vivo experiments indicate that the M35C mutation favors oligomer assembly and increases the amount of oligomers (Figure 3). The toxicity observed for AβM35C also adds further support to the notion that the methionine side chain itself is not required for toxicity, since Maiti et al.[27] have shown that a replacement of M35 by valine or norleucine still resulted in toxic Aβ. Thus, side chain modification at position 35 does not necessarily destroy the toxicity of Aβ; it is likely that the effect

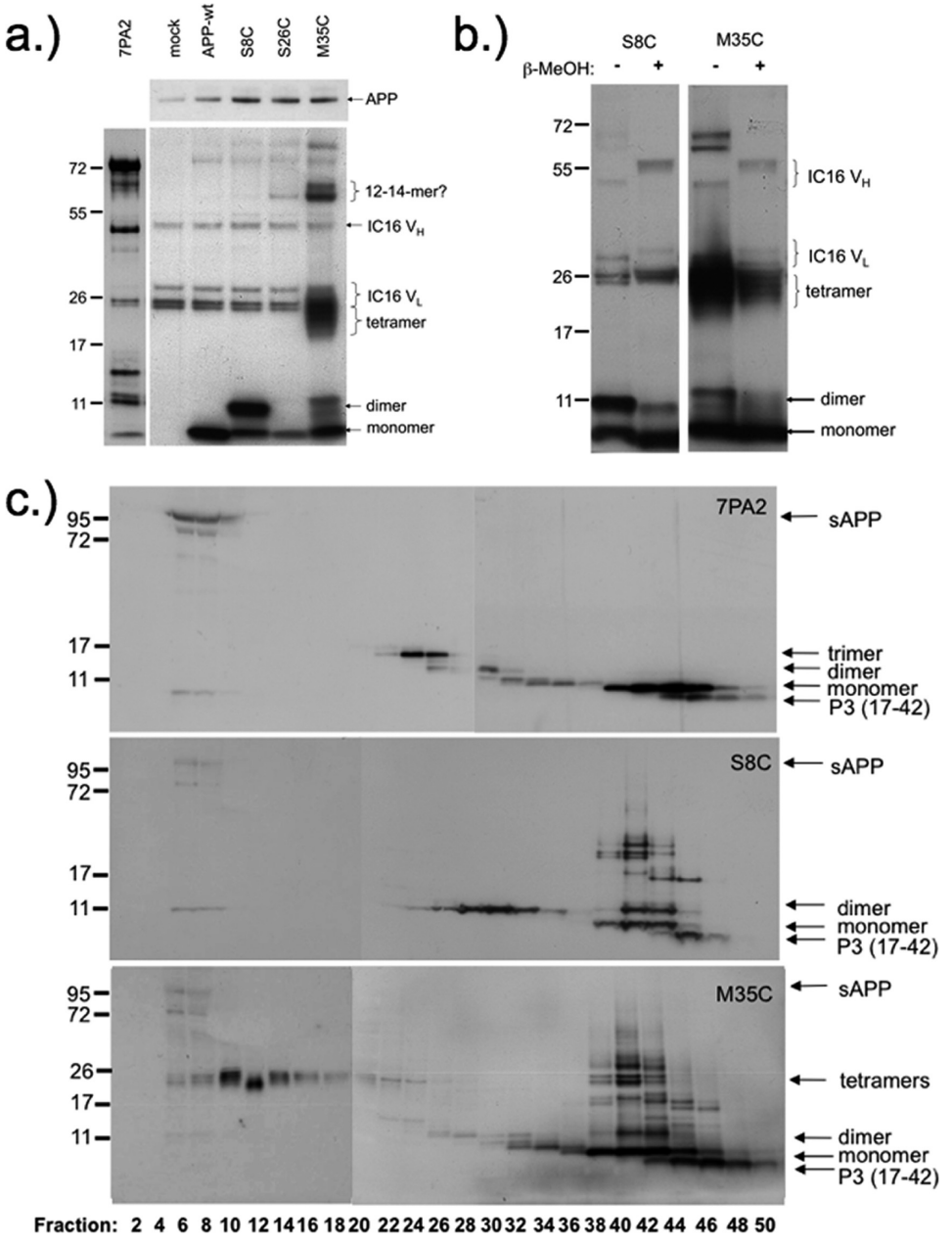

Figure 3. (a) Western blot of immunoprecipitated Aβ monomers and SDS-stable oligomers derived from SNs of permanently transfected CHO cells. Transfected CHO cells secreting the following Aβ species were used: control (mock), Aβ wildtype, AβS8C, AβS26C, or AβM35C, as indicated on top. Equal expression of APP in the cell lysates used is shown in the top panel. Only monomeric Aβ was produced by cells overexpressing APP-wt or APP(AβS26C). Predominantly dimeric Aβ, but no oligomers of higher order, was present in SNs of APP(AβS8C) cells. A heterogeneous signal pattern in the range of Aβ dimers and tetramers and putative 12−14 mers were detected in APP(AβM35C) transfected cells. Aβ was absent using empty CHO cells (mock). Detection antibody: 4G8. Additional immunoreactivity in the range of 50 and 25 kDa belongs to cross-reactivity of the secondary antibody with heavy and light chain of mAB IC16 used for immunoprecipitation. For comparison, immunoprecipitated Aβ monomers and oligomers derived from conditioned medium of 7PA2 cells (permanently secreting Aβ^{35}) are shown on the left. (b) Disulfide stabilization of Aβ dimers leads to accelerated formation of nativelike Aβ dimers. Western blot showing that a significant fraction of Aβ dimers and tetramers immunoprecipitated from AβS8C or M35C SNs remains stable after incubation in 2% β-mercaptoethanol (β-MeOH). Thus, nativelike SDS-resistant Aβ dimers are present. (c) Western blot of size exclusion chromatography (SEC) fractionated SNs from CHO cells secreting either Aβ from 7PA2 cells (top), AβS8C (middle), or AβM35C (bottom). Concentrated SNs were separated on a S75-column. Lyophilized fractions were analyzed by tricine SDS-PAGE and Western blotting using the 4G8 monoclonal antibody. With 7PA2 SN (top) a typical ladder of Aβ trimers (fractions 22−26), dimers (fr. 26−32), and monomers (fr.40−46) was seen. AβS8C (below) was only present as dimer (fr. 26−34) and monomer (fr. 40−46). In addition to dimers (fr. 26−32) and monomers (fr. 38−46), Aβ-M35C (bottom) showed signals in the range of tetrameric Aβ over a broad range between fractions 6 and 24. Higher molecular weight signals in fractions 40−46 are due to unspecific oxidations of the free cysteine in monomeric AβS8C or AβM35C with contaminants present in these fractions during the concentrating lyophilization process.

dx.doi.org/10.1021/cn200011h |*ACS Chem. Neurosci.* 2011, 2, 242–248

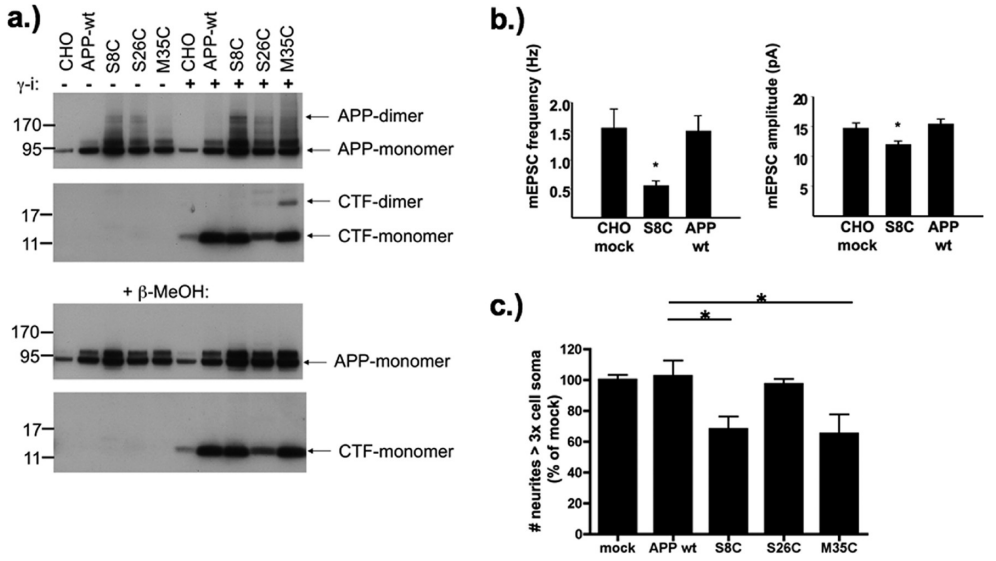

Figure 4. (a) Western blot of cell lysates derived from wt or mutant APP-overexpressing CHO cells. Western blot developed with an antibody directed against the C-terminus of APP (CT15). In contrast to CHO-mock and CHO cells expressing APP-wt, dimeric APP was present in lysates derived from cells expressing APP(AβS8C), APP(AβS26C), and APP(AβM35C) (top panel, SDS-PAGE gel run without β-MeOH). In lysates from cells treated with the γ-secretase inhibitor LY411575 (γ-i), dimeric APP-CTF was only found in cells expressing APP(AβS26C) (weak) and APP(AβM35C) constructs. Dimeric APP products were no longer visible after incubation with 2% β-MeOH, clearly demonstrating the participation of a disulfide bridge in APP dimer formation. (b) AβS8C dimers decrease miniature excitatory postsynaptic current (mEPSC) frequency and amplitude in cultured cortical neurons. mEPSC frequency and amplitude were significantly decreased in mouse primary cortical neurons incubated for 4 days with SN containing Aβ dimers (S8C; $n = 40$ cells) when compared with neurons incubated with CHO mock ($n = 39$ cells) or with the SN that was produced by CHO cells transfected with APP wt ($n = 38$ cells) that did not contain significant amounts of Aβ dimers (see Figure 3a). *$p < 0.025$ by Student's test after Bonferroni correction. Quantitative data represent mean ± SEM. (c) Purified Aβ from CHO cells expressing APP(AβS8C) and APP(AβM35C) reduced neurite outgrowth in PC12 cells. Aβ was immunoprecipitated from 5 mL supernatants of wt or APP overexpressing CHO cells. Eluted Aβ was applied to differentiating PC12 cells.[34] After 5 days, cells with neurites longer than three cell soma were quantified in 10 randomly chosen fields per well with 80−120 cells in each field. Data represent the mean ± SEM for the percentage of cell with long neurites compared to CHO mock calculated for 6 experiments. *$p < 0.05$ by ANOVA; significant decrease of neurite length after incubation with Aβ derived from CHO cells expressing APP(AβS8C) and APP(AβM35C) but not wt Aβ which did not contain significant amounts of Aβ dimers or other oligomers (see Figure 3a).

observed for oxidized M35 can be attributed to the drastic changes in polarity leading to a decreased oligomer stability. In contrast, the M35C mutation increases oligomer stability and thereby toxicity.

The ability to generate a conformationally highly homogeneous, neurotoxic, and natively secreted Aβ oligomer species has been a long-sought goal. Here, we have achieved this goal by molecular design and engineering of disulfide-bonded Aβ dimer species leading to naturally secreted, reductant-resistant Aβ dimers of relatively high yield and exclusive homogeneity. Our strategy of producing Aβ from cell lines stably expressing mutant APP avoids the labor-intensive oxidation and purification of synthetic Aβ cysteine mutants and is at the same time physiologically processed, folded, and assembled.

Our molecular dynamics simulations indicate that the AβS8C dimer adopts a structure similar to that of the wildtype and gives further support to the notion that an elongation-incompetent conformation stabilized by a hydrophobic core might be a prerequisite for Aβ dimer toxicity. Availability of large amounts of a natively secreted Aβ dimer will enable more precise studies aiming at elucidating the structure of a neurotoxic Aβ species and enable in vivo Aβ oligomer structure−activity investigations.

METHODS

Computational Studies. Molecular dynamics simulations were based on the Aβ(17−42) protofibril structure (pdb code 2BEG, model 10, chain A and B) that was obtained from NMR spectroscopic data.[28] According to previous work,[17] residues 1−16 were added to the model in an extended conformation to account for the secondary structure of Aβ(1−42) in the fibrillar form.[29] Both termini were kept ionic as under physiological conditions.

All dimer structures were electrically neutralized by the addition of an appropriate number of sodium counterions, solvated in a TIP3P[30] water box with a minimum distance of 15 Å to the border, and then subjected to a two-step restrained minimization. Because large conformational changes were expected to occur during the MD simulations, integer instead of fractional multiples of the standard Amber TIP3P water box were used resulting in large solvent boxes ($135 \times 78 \times 60$ Å^3) containing ~17.360 water molecules.

All systems were subjected to three consecutive minimizations with decreasing positional constraints, and warmed up to 300 K at a pressure of 1 bar in two stages: for 0.1 ns all peptide heavy atoms and for another 0.4 ns the peptide Cα atoms only were held fixed with a force constant of 5.0 kcal mol^{-1} Å^{-2}. After the density of the systems was close to 1.0 g/cm^3, the simulations were run without any restraints for 100.5 ns in an NPT ensemble and coordinate snapshots were collected every 50 ps. All molecular dynamics simulations were performed on the Woodcrest cluster of the Regionales Rechenzentrum Erlangen (RRZE) using Amber9[31] molecular dynamics executables optimized for parallel execution. The analysis of the resulting structures was performed as described previously.[17]

Permanently Transfected Cell Lines. For inducible expression of APP, the ORF of human APP751 was ligated into pRetroX-tight-Pur (Clontech). Cell lines were maintained in standard medium.[23]

Antibodies. Immunoprecipitation of Aβ was carried out with mAB IC16 recognizing residues 2−8 of Aβ.[23] For detection of Aβ in Western blot and cell staining, 4G8 (Signet, Dedham, MA) recognizing residues 17−24 of Aβ was used. APP and APP-CTF were visualized via polyclonal antibody CT15 recognizing the C-terminal 15 amino acids of APP.[32] The following secondary antibodies were purchased: goat anti-mouse-POD, goat anti-rabbit-POD, and Alexa-Fluor 594 conjugated goat anti-mouse IgG (Thermo Scientific, Bonn, Germany).

Immunopreciptation and Western Blot Analysis. A total of 6×10^5 cells were seeded into 10 cm cell culture dishes, and expression of APP was induced by applying 1 μg/mL doxycycline to the medium. After 3 days, cells reached confluency and supernatant was harvested. Lysis, immunoprecipitation, SDS-PAGE, and Western blotting of cleared supernatants were performed as described previously.[23] Aβ was detected using a 1:200 dilution of 4G8 and goat anti-mouse IgG (1:25 000). For detection of APP , 20 μg of the cleared lysates was separated on a NuPage 4−12% Bis/Tris gel (Invitrogen, Darmstadt, Germany) and visualized by Western blot using the polyclonal CT15 antibody (1:3500).

Size Exclusion Chromatography. To analyze the physical nature of Aβ oligomers, cells were conditioned to serum free medium after reaching confluency. Following incubation of 20 h either with doxycyclin (APP(AβS8C), APP(AβM35C)) or without (7PA2), supernatants were taken and 15× concentrated using Centriprep YM-3 (Millipore, Billerica, MA). A volume of 3 mL was injected onto a Superdex 75 prep grade column (GE, Freiburg, Germany) and eluted at 1 mL/min with 50 mM ammonium acetate pH 8.5. Lyophilized fractions of 1 mL were analyzed by Tricine-SDS-PAGE and Western blot as described above.

Culture of Cortical Mouse Neurons and Whole Cell Recordings. Cultures of cortical neurons were prepared from C57BL/6J mouse fetuses at embryonic day 18 (E18). Neurons were grown in Neurobasal A medium (GIBCO) supplemented with 2% NS-21, 100 U/mL penicillin, 100 μg/mL streptomycin, and GlutaMAX (GIBCO) on glass coverslips coated with poly-L-ornithine (1 mg/mL). After 8 days in vitro, half of the culture medium was exchanged with supernatant produced by CHO cells transfected with mutant APP releasing Aβ dimers, or with wild type APP. Whole cell recordings were perfromed as described by Jungling et al.[33] mEPSCs were recorded from cells after 4 days of incubation with supernatants, as described previously.[23]

Neurite Outgrowth Assay. Protocol was adapted from Kurz et al.[34] Aβ was immunoprecipitated by IC16-NHS-sepharose from supernatants of one confluent 10 cm dish and eluted with 100 μL of 50 mM glycine pH 2.5. Eluates were diluted 1:5 in differentiation medium (complete RPMI-1640 supplemented with 1% FCS, 1% horse serum, and 50 ng/mL NGF) and applied to 1×10^4 PC12 cells seeded 24 h before on poly-D-lysine coated 24-well plates. After 5 days, neurite outgrowth was quantified by taking 10 random photographs/well and counting of cells that developed neurites longer than three cell soma. The data are the mean ± SEM of six independent experiments.

■ ASSOCIATED CONTENT

Supporting Information. Four figures and one table showing details of the simulated structures and additional experimental properties of the Aβ dimers. This material is available free of charge via the Internet at http://pubs.acs.org.

■ AUTHOR INFORMATION

Corresponding Author

*(C.K.) Mailing address: Department Neuropathology, Heinrich Heine University Medical School, Moorenstrasse 5, 40225 Düsseldorf, Germany. Telephone: +49-211-811 6153. Fax: +49-211-811 7804. E-mail: ckorth@uni-duesseldorf.de. (H.S.) Mailing Address: Bioinformatics, Institut für Biochemie, Emil Fischer Zentrum, Friedrich-Alexander-Universität Erlangen-Nürnberg, Fahrstrasse 17, 91054 Erlangen, Germany. Telephone: +49 9131 8524614. Fax: +49 9131 8522485. E-mail: heinrich.sticht@med.uni-erlangen.de.

Author Contributions

H.S. and C.K. designed the study. H.S., C.K., and K.G. supervised the experiments. A.M-S., A.A., H.S., and A.H.C.H. performed experiments. All authors analyzed the experiments. C.K., H.S., A. H.C.H., and A.M-S. wrote the manuscript.

Funding Sources

These studies were funded by a grant from the Volkswagen-stiftung (I/82 649), Germany, awarded to C.K. and H.S and by a grant from the Stiftung für Alterforschung HHUD (C.K.).

Notes

The authors declare no conflict of interest.

■ REFERENCES

(1) Haass, C., and Selkoe, D. J. (2007) Soluble protein oligomers in neurodegeneration: lessons from the Alzheimer's amyloid beta-peptide. *Nat. Rev. Mol. Cell. Biol. 8*, 101–112.

(2) Haass, C., and Selkoe, D. J. (1993) Cellular processing of beta-amyloid precursor protein and the genesis of amyloid beta-peptide. *Cell 75*, 1039–1042.

(3) Takami, M., Nagashima, Y., Sano, Y., Ishihara, S., Morishima-Kawashima, M., Funamoto, S., and Ihara, Y. (2009) gamma-Secretase: successive tripeptide and tetrapeptide release from the transmembrane domain of beta-carboxyl terminal fragment. *J. Neurosci. 29*, 13042–13052.

(4) Naslund, J., Haroutunian, V., Mohs, R., Davis, K. L., Davies, P., Greengard, P., and Buxbaum, J. D. (2000) Correlation between elevated levels of amyloid beta-peptide in the brain and cognitive decline. *JAMA 283*, 1571–1577.

(5) McLean, C. A., Cherny, R. A., Fraser, F. W., Fuller, S. J., Smith, M. J., Beyreuther, K., Bush, A. I., and Masters, C. L. (1999) Soluble pool of Abeta amyloid as a determinant of severity of neurodegeneration in Alzheimer's disease. *Ann. Neurol. 46*, 860–866.

(6) Shankar, G. M., Li, S., Mehta, T. H., Garcia-Munoz, A., Shepardson, N. E., Smith, I., Brett, F. M., Farrell, M. A., Rowan, M. J., Lemere, C. A., Regan, C. M., Walsh, D. M., Sabatini, B. L., and Selkoe, D. J. (2008) Amyloid-beta protein dimers isolated directly from Alzheimer's brains impair synaptic plasticity and memory. *Nat. Med. 14*, 837–842.

(7) Terry, R. D., Masliah, E., Salmon, D. P., Butters, N., DeTeresa, R., Hill, R., Hansen, L. A., and Katzman, R. (1991) Physical basis of cognitive alterations in Alzheimer's disease: synapse loss is the major correlate of cognitive impairment. *Ann. Neurol. 30*, 572–580.

(8) Lambert, M. P., Barlow, A. K., Chromy, B. A., Edwards, C., Freed, R., Liosatos, M., Morgan, T. E., Rozovsky, I., Trommer, B., Viola, K. L., Wals, P., Zhang, C., Finch, C. E., Krafft, G. A., and Klein, W. L. (1998) Diffusible, nonfibrillar ligands derived from Abeta1−42 are potent central nervous system neurotoxins. *Proc. Natl. Acad. Sci. U.S.A. 95*, 6448–6453.

(9) Walsh, D. M., Klyubin, I., Fadeeva, J. V., Cullen, W. K., Anwyl, R., Wolfe, M. S., Rowan, M. J., and Selkoe, D. J. (2002) Naturally secreted oligomers of amyloid beta protein potently inhibit hippocampal long-term potentiation in vivo. *Nature 416*, 535–539.

(10) Lesne, S., Koh, M. T., Kotilinek, L., Kayed, R., Glabe, C. G., Yang, A., Gallagher, M., and Ashe, K. H. (2006) A specific amyloid-beta protein assembly in the brain impairs memory. *Nature 440*, 352–357.

(11) Barghorn, S., Nimmrich, V., Striebinger, A., Krantz, C., Keller, P., Janson, B., Bahr, M., Schmidt, M., Bitner, R. S., Harlan, J., Barlow, E.,

Ebert, U., and Hillen, H. (2005) Globular amyloid beta-peptide oligomer - a homogenous and stable neuropathological protein in Alzheimer's disease. *J. Neurochem. 95*, 834–847.

(12) Wang, Q., Walsh, D. M., Rowan, M. J., Selkoe, D. J., and Anwyl, R. (2004) Block of long-term potentiation by naturally secreted and synthetic amyloid beta-peptide in hippocampal slices is mediated via activation of the kinases c-Jun N-terminal kinase, cyclin-dependent kinase 5, and p38 mitogen-activated protein kinase as well as metabotropic glutamate receptor type 5. *J. Neurosci. 24*, 3370–3378.

(13) Petkova, A. T., Leapman, R. D., Guo, Z., Yau, W. M., Mattson, M. P., and Tycko, R. (2005) Self-propagating, molecular-level polymorphism in Alzheimer's beta-amyloid fibrils. *Science 307*, 262–265.

(14) Sandberg, A., Luheshi, L. M., Sollvander, S., Pereira de Barros, T., Macao, B., Knowles, T. P., Biverstal, H., Lendel, C., Ekholm-Petterson, F., Dubnovitsky, A., Lannfelt, L., Dobson, C. M., and Hard, T. (2010) Stabilization of neurotoxic Alzheimer amyloid-beta oligomers by protein engineering. *Proc. Natl. Acad. Sci. U.S.A. 107*, 15595–15600.

(15) Yamaguchi, T., Yagi, H., Goto, Y., Matsuzaki, K., and Hoshino, M. (2010) A disulfide-linked amyloid-beta peptide dimer forms a protofibril-like oligomer through a distinct pathway from amyloid fibril formation. *Biochemistry 49*, 7100–7107.

(16) Munter, L. M., Voigt, P., Harmeier, A., Kaden, D., Gottschalk, K. E., Weise, C., Pipkorn, R., Schaefer, M., Langosch, D., and Multhaup, G. (2007) GxxxG motifs within the amyloid precursor protein transmembrane sequence are critical for the etiology of Abeta42. *EMBO J. 26*, 1702–1712.

(17) Horn, A. H., and Sticht, H. (2010) Amyloid-beta42 oligomer structures from fibrils: a systematic molecular dynamics study. *J. Phys. Chem. B 114*, 2219–2226.

(18) Huet, A., and Derreumaux, P. (2006) Impact of the mutation A21G (Flemish variant) on Alzheimer's beta-amyloid dimers by molecular dynamics simulations. *Biophys. J. 91*, 3829–3840.

(19) Yu, L., Edalji, R., Harlan, J. E., Holzman, T. F., Lopez, A. P., Labkovsky, B., Hillen, H., Barghorn, S., Ebert, U., Richardson, P. L., Miesbauer, L., Solomon, L., Bartley, D., Walter, K., Johnson, R. W., Hajduk, P. J., and Olejniczak, E. T. (2009) Structural Characterization of a Soluble Amyloid beta-Peptide Oligomer. *Biochemistry 48*, 1870–1877.

(20) Munter, L. M., Botev, A., Richter, L., Hildebrand, P. W., Althoff, V., Weise, C., Kaden, D., and Multhaup, G. (2010) Aberrant amyloid precursor protein (APP) processing in hereditary forms of Alzheimer disease caused by APP familial Alzheimer disease mutations can be rescued by mutations in the APP GxxxG motif. *J. Biol. Chem. 285*, 21636–21643.

(21) Richter, L., Munter, L. M., Ness, J., Hildebrand, P. W., Dasari, M., Unterreitmeier, S., Bulic, B., Beyermann, M., Gust, R., Reif, B., Weggen, S., Langosch, D., and Multhaup, G. (2010) Amyloid beta 42 peptide (Abeta42)-lowering compounds directly bind to Abeta and interfere with amyloid precursor protein (APP) transmembrane dimerization. *Proc. Natl. Acad. Sci. U.S.A. 107*, 14597–14602.

(22) Eggert, S., Midthune, B., Cottrell, B., and Koo, E. H. (2009) Induced dimerization of the amyloid precursor protein leads to decreased amyloid-beta protein production. *J. Biol. Chem. 284*, 28943–28952.

(23) Muller-Schiffmann, A., Marz-Berberich, J., Andreyeva, A., Ronicke, R., Bartnik, D., Brener, O., Kutzsche, J., Horn, A. H., Hellmert, M., Polkowska, J., Gottmann, K., Reymann, K. G., Funke, S. A., Nagel-Steger, L., Moriscot, C., Schoehn, G., Sticht, H., Willbold, D., Schrader, T., and Korth, C. (2010) Combining Independent Drug Classes into Superior, Synergistically Acting Hybrid Molecules. *Angew. Chem., Int. Ed. 49*, 8743–8746.

(24) Shankar, G. M., Bloodgood, B. L., Townsend, M., Walsh, D. M., Selkoe, D. J., and Sabatini, B. L. (2007) Natural oligomers of the Alzheimer amyloid-beta protein induce reversible synapse loss by modulating an NMDA-type glutamate receptor-dependent signaling pathway. *J. Neurosci. 27*, 2866–2875.

(25) Hou, L., Shao, H., Zhang, Y., Li, H., Menon, N. K., Neuhaus, E. B., Brewer, J. M., Byeon, I. J., Ray, D. G., Vitek, M. P., Iwashita, T., Makula, R. A., Przybyla, A. B., and Zagorski, M. G. (2004) Solution NMR studies of the A beta(1−40) and A beta(1−42) peptides establish that the Met35 oxidation state affects the mechanism of amyloid formation. *J. Am. Chem. Soc. 126*, 1992–2005.

(26) Piacentini, R., Ripoli, C., Leone, L., Misiti, F., Clementi, M. E., D'Ascenzo, M., Giardina, B., Azzena, G. B., and Grassi, C. (2008) Role of methionine 35 in the intracellular Ca2+ homeostasis dysregulation and Ca2+-dependent apoptosis induced by amyloid beta-peptide in human neuroblastoma IMR32 cells. *J. Neurochem. 107*, 1070–1082.

(27) Maiti, P., Lomakin, A., Benedek, G. B., and Bitan, G. (2010) Despite its role in assembly, methionine 35 is not necessary for amyloid beta-protein toxicity. *J. Neurochem. 113*, 1252–1262.

(28) Lührs, T., Ritter, C., Adrian, M., Riek-Loher, D., Bohrmann, B., Dobeli, H., Schubert, D., and Riek, R. (2005) 3D structure of Alzheimer's amyloid-beta(1−42) fibrils. *Proc. Natl. Acad. Sci. U.S.A. 102*, 17342–17347.

(29) Olofsson, A., Sauer-Eriksson, A. E., and Ohman, A. (2006) The solvent protection of alzheimer amyloid-beta-(1−42) fibrils as determined by solution NMR spectroscopy. *J. Biol. Chem. 281*, 477–483.

(30) Jorgensen, W. L., Chandrasekhar, J., Madura, J. D., Impey, R. W., and Klein, M. L. (1983) Comparison of simple potential functions for simulationg liquid water. *J. Chem. Phys. 79*, 926–935.

(31) Case, D. A.; Darden, T. A.; Cheatham, T. E.; Simmerling, C. L.; Wang, J.; Duke, R. E.; Luo, R.; Merz, K. M.; Pearlman, D. A.; Crowley, M.; Walker, R. C.; Zhang, W.; Wang, B.; Hayik, S.; Roitberg, A.; Seabra, G.; Wong, K. F.; Paesani, F.; Wu, X.; Brozell, S.; Tsui, V.; Gohlke, H.; Yang, L.; Tan, C.; Mongan, J.; Hornak, V.; Cui, G.; Beroza, P.; Mathews, D. H.; Schafmeister, C.; Ross, W. S.; Kollman, P. A. (2006) *AMBER9*, University of California, San Francisco.

(32) Sisodia, S. S., Koo, E. H., Hoffman, P. N., Perry, G., and Price, D. L. (1993) Identification and transport of full-length amyloid precursor proteins in rat peripheral nervous system. *J. Neurosci. 13*, 3136–3142.

(33) Jungling, K., Eulenburg, V., Moore, R., Kemler, R., Lessmann, V., and Gottmann, K. (2006) N-cadherin transsynaptically regulates short-term plasticity at glutamatergic synapses in embryonic stem cell-derived neurons. *J. Neurosci. 26*, 6968–6978.

(34) Kurz, C., Ungerer, I., Lipka, U., Kirr, S., Schutt, T., Eckert, A., Leuner, K., and Muller, W. E. (2010) The metabolic enhancer piracetam ameliorates the impairment of mitochondrial function and neurite outgrowth induced by beta-amyloid peptide. *Br. J. Pharmacol. 160*, 246–257.

(35) Podlisny, M. B., Ostaszewski, B. L., Squazzo, S. L., Koo, E. H., Rydell, R. E., Teplow, D. B., and Selkoe, D. J. (1995) Aggregation of secreted amyloid beta-protein into sodium dodecyl sulfate-stable oligomers in cell culture. *J. Biol. Chem. 270*, 9564–9570.